

Multiple dark-bright solitons in atomic Bose-Einstein condensatesD. Yan,¹ J. J. Chang,² C. Hamner,² P. G. Kevrekidis,¹ P. Engels,² V. Achilleos,³ D. J. Frantzeskakis,³
R. Carretero-González,^{4,*} and P. Schmelcher⁵¹*Department of Mathematics and Statistics, University of Massachusetts, Amherst, Massachusetts 01003-4515, USA*²*Department of Physics and Astronomy, Washington State University, Pullman, Washington 99164, USA*³*Department of Physics, University of Athens, Panepistimiopolis, Zografos, GR-157 84 Athens, Greece*⁴*Nonlinear Dynamical Systems Group, Department of Mathematics and Statistics and Computational Science Research Center, San Diego State University, San Diego, California 92182-7720, USA*⁵*Zentrum für Optische Quantentechnologien, Universität Hamburg, Luruper Chaussee 149, D-22761 Hamburg, Germany*
(Received 21 April 2011; published 28 November 2011)

Motivated by recent experimental results, we present a systematic theoretical analysis of dark-bright-soliton interactions and multiple-dark-bright-soliton complexes in atomic two-component Bose-Einstein condensates. We study analytically the interactions between two dark-bright solitons in a homogeneous condensate and then extend our considerations to the presence of the trap. We illustrate the existence of robust stationary dark-bright-soliton “molecules,” composed of two or more solitons, which are formed due to the competition of the interaction forces between the dark- and bright-soliton components and the trap force. Our analysis is based on an effective equation of motion, derived for the distance between two dark-bright solitons. This equation provides equilibrium positions and characteristic oscillation frequencies of the solitons, which are found to be in good agreement with the eigenfrequencies of the anomalous modes of the system.

DOI: [10.1103/PhysRevA.84.053630](https://doi.org/10.1103/PhysRevA.84.053630)

PACS number(s): 03.75.Mn, 05.45.Yv, 03.75.Kk

I. INTRODUCTION

Over the past few years, the macroscopic nonlinear structures that can be supported in atomic Bose-Einstein condensates (BECs) have been a topic of intense investigation (see, e.g., Refs. [1–4] for reviews of this topic). The first experimental efforts to identify the predominant nonlinear structure in BECs with repulsive interatomic interactions, namely the dark soliton, were initiated over a decade ago [5–9]. However, these efforts suffered from a number of instabilities arising due to dimensionality and/or temperature effects. More recently, a new generation of relevant experiments has emerged that has enabled overcoming (or quantification of) some of the above limitations. The latter works have finally realized oscillating, and even interacting, robust dark solitons in atomic BECs. This has been achieved by means of various techniques, including phase-imprinting and density engineering [10–12], matter-wave interference [13,14], and dragging localized defects through the BECs [15].

Atomic dark solitons may also exist in multicomponent condensates, where they are coupled to other nonlinear macroscopic structures [1,2,4]. Of particular interest are dark-bright (DB) solitons that are supported in two-component [16] and spinor [17] condensates. Such structures are sometimes referred to as “symbiotic” solitons, as the bright-soliton component (which is generically supported in BECs with attractive interactions [3]) may only exist due to the interspecies interaction with the dark-soliton component. Dark-bright solitons have also attracted much attention in other contexts, such as nonlinear optics [18] and mathematical physics [19]. In fact, DB-soliton states were first observed in optics experiments, where they were created in photorefractive crystals [20], while their interactions were partially monitored

in Ref. [21]. In the physics of BECs, robust DB solitons were first observed in the experiment of Ref. [10] by means of a phase-imprinting method, and they were observed more recently in Refs. [22–24] by means of the counterflow of the two BEC components. The above efforts led to a renewed interest in theoretical aspects of this theme: in this way, DB-soliton interactions were studied from the viewpoint of the integrable systems theory in Ref. [25], DB-soliton dynamics were investigated numerically in Ref. [26], and DB solitons in discrete settings were recently analyzed in Ref. [27]. Furthermore, higher-dimensional generalizations, namely, vortex-bright-soliton structures, were studied as well [28].

Our aim in the present work is to study multiple-DB solitons in two-component BECs confined in harmonic traps, as motivated by the experimental results shown in Fig. 1. Figure 1 illustrates DB-soliton clustering occurring during the counterflow of two rubidium condensate species, namely, the hyperfine states $|1, -1\rangle$ and $|2, -2\rangle$, confined in an elongated optical dipole trap with measured trap frequencies of $2\pi\{1.5, 140, 178\}$ Hz; details on the soliton generation scheme are provided in Refs. [22–24]. An intriguing observation is the frequent formation of large gaps in one component (which constitutes the component supporting the dark solitons) that are filled by bright solitons in the other component. Interestingly, these gaps are structured by small, periodic density bumps, indicating that these regions are composed of merged solitons. Some of these features are marked by the boxed regions in Fig. 1, with corresponding cross sections shown as insets. We clearly observe clusters of two and three merged solitons [see Figs. 1(a)–1(c)] and also have some indications of clusters composed of four to five solitons; see Figs. 1(d) and 1(e). While our destructive imaging technique does not allow us to analyze the dynamics and lifetime of the clusters in detail, the occurrence of large DB-soliton clusters strongly supports the theoretical part of our work that we will present below: we will

*<http://nlds.sdsu.edu>

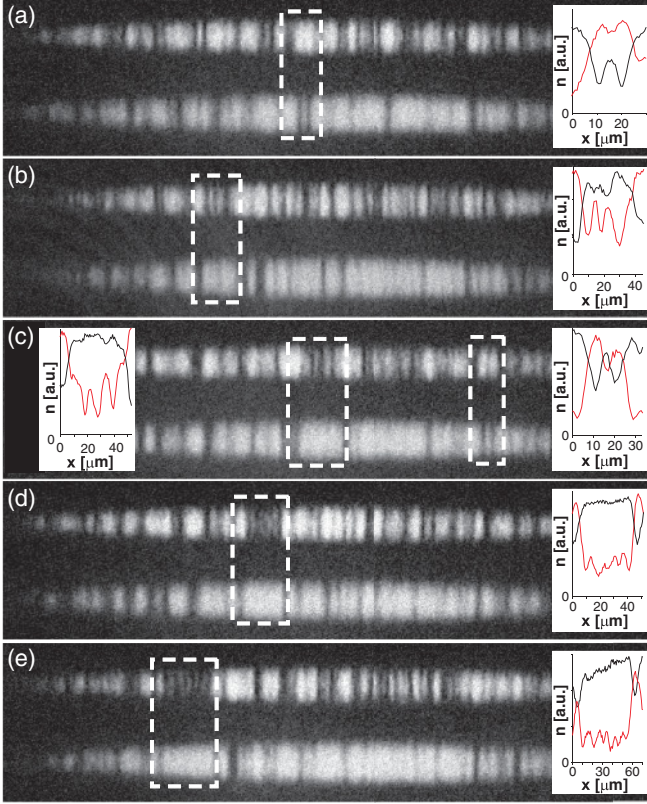


FIG. 1. (Color online) Experimental images indicating DB-soliton clustering in a two-component BEC. The upper cloud in each image [and the red (gray) curve in the inset] shows atoms in the $|2, -2\rangle$ state, while the lower cloud (black curve) shows atoms in the $|1, -1\rangle$ state. Prior to imaging, the two components are overlapped in the trap for 5 s. Insets show integrated cross sections of the boxed regions.

study analytically the interaction between two DB solitons, and we will demonstrate the existence of stable two- and multiple-DB stationary states, resembling the ones observed in the experiment.

Our analytical approximation relies on a Hamiltonian perturbation theory, which leads to an equation of motion of the centers of DB-soliton interacting pairs. Employing this equation of motion, we demonstrate the existence of robust DB-soliton molecules, in the form of stationary two- and three-DB-soliton states. We also find semianalytically the equilibrium distance of the constituent solitons as well as the oscillation frequencies around these equilibria. The oscillation frequencies correspond to the characteristic anomalous modes' eigenfrequencies that we numerically compute via a Bogoliubov–de Gennes (BdG) analysis. In this way, we are able to quantify the properties of stationary multiple DB solitons in harmonically confined two-component BECs and provide analytical results for their in- and out-of-phase near-equilibrium motions.

This paper is organized as follows. In Sec. II we describe our theoretical setup and present the DB-soliton states. Section III is devoted to the study of the interactions of two DB solitons, while Sec. IV contains the results for multiple DB solitons in the trap. In all of these sections, we will

first present our theoretical analysis, and subsequently, we will compare its predictions to numerical results. Finally, in Sec. V we summarize our findings and discuss future challenges.

II. MODEL AND THEORETICAL SETUP

A. Coupled Gross-Pitaevskii equations and dark-bright solitons

Following the experimental observations of the previous section, we consider a two-component elongated (along the x direction) BEC composed of two different hyperfine states of rubidium. As is the case of the experiment, we consider a highly anisotropic trap, with the longitudinal and transverse trapping frequencies such that $\omega_x \ll \omega_\perp$. In the framework of the mean-field theory, the dynamics of this two-component BEC can be described by the following system of two coupled Gross-Pitaevskii equations [1,2,4]:

$$i\hbar\partial_t\psi_j = \left(-\frac{\hbar^2}{2m}\partial_x^2\psi_j + V(x) - \mu_j + \sum_{k=1}^2 g_{jk}|\psi_k|^2 \right) \psi_j. \quad (1)$$

Here $\psi_j(x,t)$ ($j = 1,2$) denote the mean-field wave functions of the two components (normalized to the numbers of atoms $N_j = \int_{-\infty}^{+\infty} |\psi_j|^2 dx$), m is the atomic mass, μ_j are the chemical potentials, and $V(x)$ represents the external harmonic trapping potential, $V(x) = (1/2)m\omega_x^2 x^2$. In addition, $g_{jk} = 2\hbar\omega_\perp a_{jk}$ are the effective one-dimensional (1D) coupling constants, where a_{jk} denote the three s -wave scattering lengths (note that $a_{12} = a_{21}$) accounting for collisions between atoms belonging to the same (a_{jj}) or different ($a_{jk}, j \neq k$) species. In the case of the hyperfine states $|1, -1\rangle$ and $|2, -2\rangle$ of ^{87}Rb considered in the previous section, the scattering lengths take the values $a_{11} = 100.4a_0$, $a_{12} = 98.98a_0$ and $a_{22} = 98.98a_0$ (where a_0 is the Bohr radius) [22,23]. Thus, we will hereafter use the approximation that all scattering lengths take the same value, say $a_{ij} \approx a$ [29]. To this end, measuring the densities $|\psi_j|^2$, length, time, and energy in units of $2a$, $a_\perp = \sqrt{\hbar}/\omega_\perp$, ω_\perp^{-1} , and $\hbar\omega_\perp$, respectively, we may reduce the system of Eqs. (1) into the following dimensionless form:

$$i\partial_t\psi_j = -\frac{1}{2}\partial_x^2\psi_j + V(x)\psi_j + (|\psi_j|^2 + |\psi_{3-j}|^2 - \mu_j)\psi_j, \quad (2)$$

$$j = 1,2,$$

where the external potential in Eq. (2) is given by $V(x) = (1/2)\Omega^2 x^2$, where $\Omega = \omega_x/\omega_\perp \ll 1$ is the normalized trap strength. Below, we will consider a situation where the component characterized by the wave function ψ_1 (ψ_2) supports a single or a multiple dark (bright) soliton state, and the respective chemical potentials will be such that $\mu_1 > \mu_2$. As concerns the component ψ_1 , the dark-soliton state exists on top of a ground-state cloud $|\psi_{\text{GS}}|^2$, which for appropriately large values of μ_1 can be approximated by the Thomas-Fermi (TF) density $|\psi_{\text{GS}}|^2 \approx |\psi_{\text{TF}}|^2 = \mu_1 - V(x)$; thus, to describe the dark-soliton wave function, we substitute the density $|\psi_1|^2$ in Eq. (2) as $|\psi_1|^2 \rightarrow |\psi_{\text{TF}}|^2 |\psi_1|^2$. Furthermore, we introduce the transformations $t \rightarrow \mu_1 t$, $x \rightarrow \sqrt{\mu_1} x$, $|\psi_2|^2 \rightarrow \mu_1^{-1} |\psi_2|^2$

and cast Eq. (2) into the following form:

$$i \partial_t \psi_1 + \frac{1}{2} \partial_x^2 \psi_1 - (|\psi_1|^2 + |\psi_2|^2 - 1) \psi_1 = R_1, \quad (3)$$

$$i \partial_t \psi_2 + \frac{1}{2} \partial_x^2 \psi_2 - (|\psi_1|^2 + |\psi_2|^2 - \tilde{\mu}) \psi_2 = R_2, \quad (4)$$

where $\tilde{\mu} = \mu_2/\mu_1$, while

$$\begin{aligned} R_1 &\equiv (2\mu_1^2)^{-1} [2(1 - |\psi_1|^2)V(x)\psi_1 + V'(x)\partial_x\psi_1], \\ R_2 &\equiv \mu_1^{-2} [(1 - |\psi_1|^2)V(x)\psi_2], \end{aligned} \quad (5)$$

with $V'(x) \equiv dV/dx$. Equations (3) and (4) can be viewed as a system of two coupled perturbed nonlinear Schrödinger (NLS) equations, with perturbations given by Eqs. (5). In the absence of the trap (i.e., for $\Omega = 0$), the perturbations vanish, and Eqs. (3) and (4) actually constitute the completely integrable Manakov case [30]. This system conserves, among other quantities, the Hamiltonian (total energy),

$$\begin{aligned} E &= \frac{1}{2} \int_{-\infty}^{+\infty} \mathcal{E} dx, \\ \mathcal{E} &= |\partial_x \psi_1|^2 + |\partial_x \psi_2|^2 + (|\psi_1|^2 + |\psi_2|^2 - 1)^2 \\ &\quad - 2(\tilde{\mu} - 1)|\psi_2|^2, \end{aligned} \quad (6)$$

as well as the total number of atoms, $N = N_1 + N_2 = \sum_{j=1}^2 \int_{-\infty}^{+\infty} |\psi_j|^2 dx$; additionally, the number of atoms of each component, N_1 and N_2 , is separately conserved.

Considering the boundary conditions $|\psi_1|^2 \rightarrow 1$ and $|\psi_2|^2 \rightarrow 0$ as $|x| \rightarrow \infty$, the NLS equations (3) and (4) possess an exact analytical single-DB-soliton solution of the following form (see, e.g., Ref. [16]):

$$\psi_1(x, t) = \cos \phi \tanh\{D[x - x_0(t)]\} + i \sin \phi, \quad (7)$$

$$\psi_2(x, t) = \eta \operatorname{sech}\{D[x - x_0(t)]\} \exp[ikx + i\theta(t)], \quad (8)$$

where ϕ is the dark soliton's phase angle, $\cos \phi$ and η represent the amplitudes of the dark and bright solitons, D and $x_0(t)$ denote the inverse width and the center of the DB soliton, and $k = D \tan \phi = \text{const}$ and $\theta(t)$ are the wave number and phase of the bright soliton, respectively. The soliton parameters are connected through the following equations:

$$D^2 = \cos^2 \phi - \eta^2, \quad (9)$$

$$\dot{x}_0 = D \tan \phi, \quad (10)$$

$$\theta(t) = \frac{1}{2}(D^2 - k^2)t + (\tilde{\mu} - 1)t, \quad (11)$$

where $\dot{x}_0 = dx_0/dt$ is the DB soliton velocity. Below, we will mainly focus on stationary solutions, characterized by a dark soliton's phase angle $\phi = 0$ [in this case, the bright-soliton component is stationary as well; see Eq. (10)]; nevertheless, we will also consider the near-equilibrium motion of DB solitons, characterized by $\phi \approx 0$.

To approximate a two-DB-soliton state (for $\Omega = 0$) composed of a pair of two equal-amplitude single DB solitons traveling in opposite directions, we will use the following ansatz:

$$\begin{aligned} \psi_1(x, t) &= (\cos \phi \tanh X_- + i \sin \phi) \\ &\quad \times (\cos \phi \tanh X_+ - i \sin \phi), \end{aligned} \quad (12)$$

$$\begin{aligned} \psi_2(x, t) &= \eta \operatorname{sech} X_- e^{i[+kx + \theta(t) + (\tilde{\mu} - 1)t]} \\ &\quad + \eta \operatorname{sech} X_+ e^{i[-kx + \theta(t) + (\tilde{\mu} - 1)t]} e^{i\Delta\theta}, \end{aligned} \quad (13)$$

where $X_{\pm} = D[x \pm x_0(t)]$, $2x_0$ is the relative distance between the two solitons, and $\Delta\theta$ is the relative phase between the two bright solitons, assumed to be constant ($\Delta\theta = 0$ and $\Delta\theta = \pi$ correspond to in-phase and out-of-phase bright solitons, respectively). Notice that ansatz (12) is a symmetric form of two dark solitons on the common background that, provided that the separation distance $2x_0$ is sufficiently large, weakly interact with each other; such an ansatz for the dark-soliton pair has been used for the study of the intersoliton interactions [31]. Similarly, ansatz (13) is a superposition of two bright solitons of equal amplitudes, placed at the locations of their respective dark-soliton siblings; such a form of the bright-soliton pair is commonly used for the study of interactions between bright solitons (see, e.g., Chap. 3.2.2 of Ref. [18]).

At this point it is useful to note that in either case of single or multiple DB solitons, the number of atoms of the bright soliton N_2 may be used to connect the amplitude η of the bright soliton(s), the chemical potential μ_1 of the dark-soliton component, and the inverse width D of the DB soliton. In particular, in the case of a single DB soliton, one finds that $N_2 = 2\eta^2 \sqrt{\mu_1}/D$ [for the variables appearing in Eq. (2)], while for the case of a two-DB-soliton state (with well-separated solitons) the relevant result is approximately twice as large, namely,

$$N_2 \approx \frac{4\eta^2 \sqrt{\mu_1}}{D}. \quad (14)$$

B. Stationary states and their excitation spectrum

Apart from our analytical approximations, we will also use numerical methods to obtain stationary DB-soliton states and determine their stability by means of the well-known BdG analysis (see, e.g., Refs. [1,2,4]). Particularly, in our numerical computations below, we will initially obtain, by means of a fixed-point algorithm, stationary solutions of Eq. (2) in the form $\psi_1(x, t) = u(x)$ and $\psi_2(x, t) = v(x)$, and then we will consider their linear stability, upon introducing the following ansatz into Eq. (2):

$$\psi_1(x, t) = u(x) + \varepsilon[a(x)e^{\lambda t} + b^*(x)e^{\lambda^* t}], \quad (15)$$

$$\psi_2(x, t) = v(x) + \varepsilon[c(x)e^{\lambda t} + d^*(x)e^{\lambda^* t}], \quad (16)$$

where the asterisk denotes complex conjugation. The resulting equations are linearized (keeping only terms of order of the small parameter ε), and the ensuing eigenvalue problem for eigenmodes $\{a(x), b(x), c(x), d(x)\}$ and eigenvalues $\lambda = \lambda_r + i\lambda_i$ is numerically solved. In the case of a single DB soliton, the excitation spectrum can be well understood in both cases, corresponding to the absence and the presence of the harmonic trap, using the following arguments.

First, in the absence of the trap, the system of Eq. (2) features not only a U(1) (phase) invariance in each of the components but also a translational invariance; thus, the system has three pairs of eigenvalues (each associated with one of the above symmetries) at the origin of the spectral plane (λ_r, λ_i). In this case, the phonon band (associated with the continuous spectrum of the problem) covers the entire imaginary axis of the spectral plane.

Second, in the presence of the trap, the single DB soliton “lives” on the background of the confined ground state $\{\psi_1, \psi_2\} = \{\psi_{\text{GS}}, 0\}$ (as discussed above). It is well known [1,2] that the harmonic potential introduces a discrete (point) BdG spectrum for this spatially confined ground state. In addition to that, the translational invariance of the unconfined system is broken, and due to the presence of the DB soliton, a single eigenvalue $\lambda^{(\text{AM})}$ emerges. The respective (negative energy) eigenmode is the so-called anomalous mode (AM), while the associated eigenvalue $\lambda^{(\text{AM})}$ is directly connected with the oscillation frequency of the DB soliton in the harmonic trap, similar to the case of a dark soliton in one-component BECs [32]. In fact, the imaginary part of the eigenvalue $\lambda^{(\text{AM})}$ reads $\lambda_i^{(\text{AM})} = \omega_{\text{osc}}$, where ω_{osc} is the oscillation frequency of the single DB soliton, given by [16]

$$\omega_{\text{osc}}^2 = \Omega^2 \left(\frac{1}{2} - \frac{\chi}{\chi_0} \right), \quad (17)$$

$$\chi \equiv \frac{N_2}{\sqrt{\mu_1}}, \quad \chi_0 \equiv 8\sqrt{1 + \left(\frac{\chi}{4}\right)^2}. \quad (18)$$

The above results are illustrated in Fig. 2, where a typical example of a stationary single-DB-soliton state has been numerically computed and is depicted (top panel); additionally, the eigenvalues λ_i characterizing the numerically obtained excitation (BdG) spectra of such stationary states are shown as functions of the chemical potentials μ_1 and μ_2 in the middle and bottom panels of Fig. 2, respectively. As observed in the middle and bottom panels, there exist two types of spectral lines, namely, “slowly varying” ones (analogous to ones that are present in the spectrum of a dark soliton in one-component BECs [13]) and “rapidly varying” ones due to the presence of the bright-soliton component. The latter, as was pointed out also in Ref. [24], may, in fact, collide with the internal anomalous mode of the DB soliton and give rise to instability quartets, which are barely discernible in Fig. 2 (see, e.g., the bottom panel for $\mu_2 > 1.4$, where a merger of eigenvalues occurs). Generally, however, it is found that the analytical prediction (red dashed line) is *excellent* in capturing the anomalous mode eigenvalue pertaining to the DB-soliton oscillation.

The above discussion sets the stage for the presentation of our results for multiple-DB-soliton states.

III. INTERACTION BETWEEN TWO DARK-BRIGHT SOLITONS

We start with the case where the external trap is absent, i.e., $\Omega = 0$. To analytically study the interaction of two identical DB solitons, cf. Eqs. (12) and (13), we will employ the adiabatic approximation of the perturbation theory for matter-wave solitons (see, e.g., Refs. [2,4]). In particular, we assume that the approximate two-DB-soliton state features an adiabatic evolution due to a weak mutual interaction between the constituent solitons, and thus, the DB soliton parameters become slowly varying unknown functions of time t . Thus, $\phi \rightarrow \phi(t)$, $D \rightarrow D(t)$, and hence, Eqs. (9) and (10) become

$$D^2(t) = \cos^2 \phi(t) - \frac{1}{4}\chi D(t), \quad (19)$$

$$\dot{x}_0(t) = D(t) \tan \phi(t), \quad (20)$$

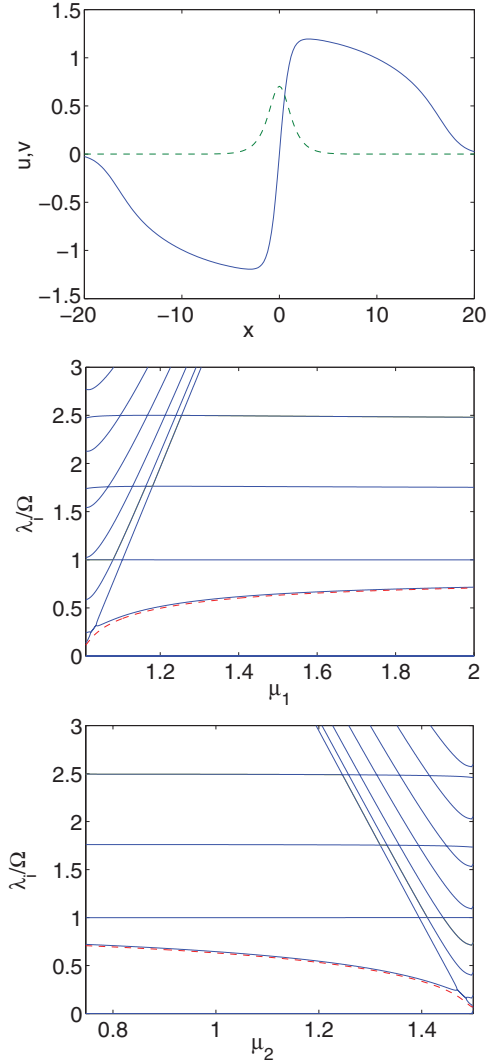


FIG. 2. (Color online) The top panel depicts the stationary solution for a single DB soliton for $\mu_1 = 3/2$, $\mu_2 = 1$, and $\Omega = 0.1$. The bright (dark) components are shown by the dashed green (solid blue) line. The middle (bottom) panel shows the normalized imaginary part λ_i/Ω of the eigenvalues for the single DB soliton as a function of μ_1 (μ_2) for $\mu_2 = 1$ ($\mu_1 = 3/2$). The red dashed line depicts the analytical prediction of Ref. [16] for the DB-soliton oscillation frequency [cf. Eq. (17)], providing an excellent approximation to the anomalous mode eigenfrequency.

where we have used Eq. (14). The evolution of the parameters $\phi(t)$, $D(t)$, and $x_0(t)$ can then be found by means of the evolution of the DB-soliton energy as follows. First, we substitute the ansatz (12) and (13) into Eq. (6) and perform the integrations under the assumption that the soliton velocity is sufficiently small, such that $\cos(kx) \approx 1$ [and $\sin(kx) \approx 0$]. Then, we further simplify the result assuming that the solitons are well separated, i.e., their relative distance is $x_0 \gg 1$. In this way, we find, by substitution of the trial ansatz of Eqs. (12) and (13) into the total energy of the system given by Eq. (6), that the latter assumes the form

$$E = 2E_1 + E_{\text{DD}} + E_{\text{BB}} + 2E_{\text{DB}}, \quad (21)$$

where E_1 is the energy of a single DB soliton, namely,

$$E_1 = \frac{4}{3}D^3 + \eta^2 \left(\frac{k^2 - 2(\tilde{\mu} - 1)}{D} + D \right), \quad (22)$$

while the remaining terms account for the interaction between the two DB solitons. In particular, E_{DD} , E_{BB} , and E_{DB} denote, respectively, the interaction energy between the two dark solitons, the interaction energy between the two bright ones, and the interaction energy between the dark soliton of one component and the bright soliton in the other component. Approximate expressions for the above interaction energies are provided in the Appendix.

Having determined the two-DB-soliton energy, we can find the evolution of the soliton parameters from the energy conservation, $dE/dt = 0$. We focus on the case of low-velocity, almost-black solitons [with $\dot{D}(t) \approx 0$ and $\cos\phi(t) \approx 1$], for which energy conservation leads to the following nonlinear evolution equation for the DB soliton center:

$$\ddot{x}_0 = F_{\text{int}}, \quad (23)$$

$$F_{\text{int}} \equiv F_{DD} + F_{BB} + 2F_{DB}. \quad (24)$$

In the above equations, F_{int} is the interaction force between the two DB solitons (depending on the soliton coordinate x_0), which contains the following three distinct contributions: the interaction forces F_{DD} and F_{BB} between the two dark and two bright solitons, respectively, and the interaction force F_{DB} of the dark soliton of the one soliton pair with the bright soliton of the other pair. The functional form of the above forces is provided in the Appendix.

The equation of motion for the two-DB-soliton state [cf. Eq. (23)] provides a clear physical picture for the interaction between the two DB solitons. In order to better understand this result, first we note that (to the leading order of approximation) the interaction force between the bright-soliton components introduces a longer-range effect than the interaction forces between the dark-soliton components, which in turn introduces a shorter-range repulsion. This can be seen since $F_{BB} \propto \exp(-2D_0x_0)$ and $F_{DD} \propto \exp(-4D_0x_0)$ (see the Appendix); note that the interaction between dark and bright solitons is also to leading order, $F_{DB} \propto \exp(-2D_0x_0)$. This result is in accordance with earlier predictions, where the same dependence of the force over the soliton separation was found (see, e.g., Refs. [33] and [14,31,34] for bright and dark solitons, respectively).

Let us now consider the role of the bright-soliton component. In its absence, i.e., for $\chi = 0$ [cf. Eq. (19)], it is clear that $F_{BB} = F_{DB} = 0$ and Eq. (23) describes the interaction between two dark (almost black) solitons; in this case, taking into account that $D_0 = 1$, it can readily be found that the pertinent (repulsive) interaction potential is $\propto 2 \exp(-4x_0)$, which coincides with the result of Ref. [31] (see also Refs. [4,14]). On the other hand, when bright solitons are present (i.e., for $\chi \neq 0$), the principal nature of the bright-bright-soliton interaction, and also of part of the dark-bright-soliton interaction, depends on the relative phase $\Delta\theta$ between the two bright solitons through the factor $\cos\Delta\theta$; see also Eqs. (A5) and (A6) in the Appendix. In particular, if $\Delta\theta = 0$ (in-phase case), the interaction is repulsive, while if $\Delta\theta = \pi$ (out-of-phase case), the interaction is attractive [35].

According to the above, it is clear that the competition between repulsive (for dark solitons) and attractive (for out-of-phase bright solitons) forces leads to the emergence of fixed points in the equation of motion (23) [36]. In other words, in this case, there exists a *stationary* DB-soliton “molecule” composed of two DB solitons. Note that stationary two DB solitons were also found numerically and experimentally in Ref. [21] in the context of nonlinear optics, but their existence details and stability properties were not considered. Additionally, although exact two-DB-soliton solutions (as well as \mathcal{N} -DB-soliton solutions) do exist in the Manakov system [25,37], their complicated form does not allow for a transparent physical picture, as provided above.

The fixed (equilibrium) points x_{eq} of Eq. (23), which represent the equilibrium distance between the constituent DB solitons forming the stationary molecule, can be determined as solutions of the transcendental equation resulting from Eq. (23) for $\ddot{x}_0 = 0$ in the out-of-phase case ($\Delta\theta = \pi$). Once x_{eq} are found, their stability can be studied by introducing the ansatz $x_0(t) = x_{\text{eq}} + \delta(t)$ into Eq. (23) and linearizing with respect to the small-amplitude perturbation $\delta(t)$; in this way, we derive the following equation:

$$\ddot{\delta} + \omega_0^2 \delta = 0, \quad (25)$$

where the oscillation frequency ω_0 is given by

$$\omega_0^2 = - \left. \frac{\partial F_{\text{int}}}{\partial x_0} \right|_{x_0=x_{\text{eq}}}. \quad (26)$$

Physically speaking, the oscillation frequency ω_0 represents the internal out-of-phase motion of the two DB solitons. Note that, as here we deal with the homogeneous case (i.e., in the absence of the trap), the in-phase motion of the solitons is associated with the neutral translation mode due to the translational invariance of the system (the respective in-phase Goldstone mode has a vanishing frequency).

The above analytical predictions have been compared with numerical simulations. First, we have confirmed the existence of the stationary two-DB-soliton state (in the out-of-phase case); a prototypical example of such a state is shown in the top panel of Fig. 3 (for $\mu_1 = 3\mu_2/2 = 3/2$). We have also determined the dependence of the equilibrium soliton positions (denoted by x_0 in the middle panel of Fig. 3) and the effective frequency ω_0 [cf. Eq. (26)] on the chemical potential μ_2 of the bright-soliton component. The respective analytical and numerical results are shown in the middle and bottom panels of Fig. 3. To obtain the numerical results, we have used a (least-squares) fitting algorithm to accurately identify the amplitude η , inverse width D , and equilibrium center of mass position x_0 of the bright component. The numerical findings for x_0 and ω_0 (the latter is numerically obtained via a BdG analysis, as the imaginary eigenvalue λ_i pertaining to the out-of-phase motion of the stationary two-DB-soliton state) are directly compared with the semianalytical results of Eqs. (23) and (26), respectively. We find that there is a very good quantitative agreement between the analytical and numerical results (see middle and bottom panels of Fig. 3). Notice that despite the motion of this eigenvalue through the continuous spectrum, no instability is observed in the parametric window shown in Fig. 3.

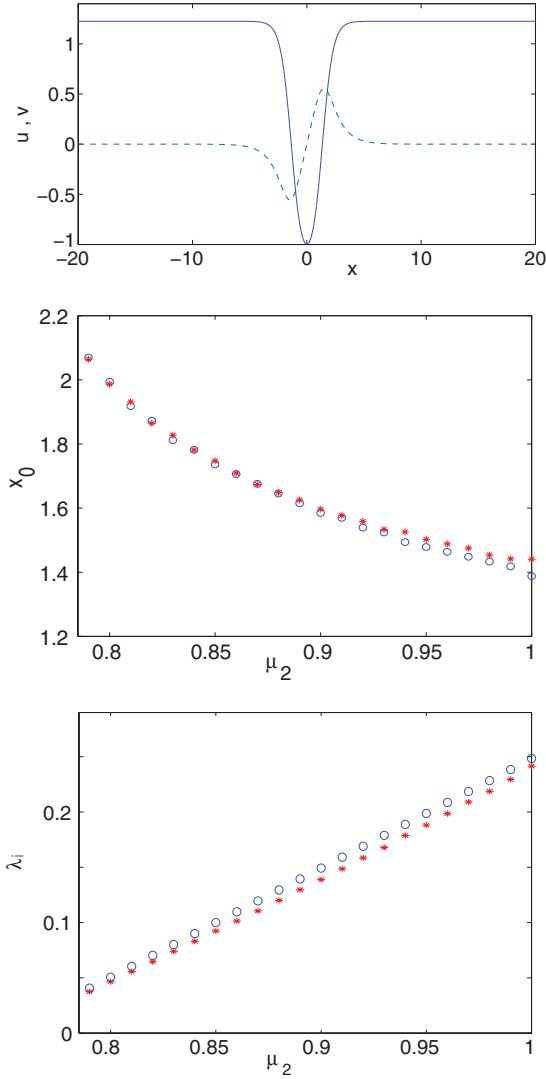


FIG. 3. (Color online) (top) A stationary DB-soliton pair: the solid blue line denotes the two-dark-soliton state (recall that each dark soliton is associated with a zero crossing), while the dashed green line denotes the respective two-bright-soliton state. The chemical potentials are $\mu_1 = 3/2$ and $\mu_2 = 1$. (middle) The equilibrium center of mass x_0 as a function of the chemical potential μ_2 (for $\mu_1 = 3/2$). Red stars denote the analytical prediction of Eq. (23), while blue circles denote the numerically obtained soliton center x_0 . (bottom) The oscillation frequency for the out-of-phase motion of the DB-soliton pair as a function of μ_2 (for $\mu_1 = 3/2$). Red stars depict the analytical result for ω_0 [cf. Eq. (26)], while blue circles depict the corresponding numerically obtained imaginary eigenvalue λ_i (for the out-of-phase soliton motion) of the excitation spectrum.

IV. MULTIPLE DARK-BRIGHT SOLITONS IN THE TRAP

Next, let us consider the case of multiple DB solitons in the presence of the harmonic trap. In the presence of the trap, each of the multiple-DB-soliton structures is subject to two forces: (a) the restoring force of the trap F_{tr} [in the case of a single DB soliton, this force induces an in-trap oscillation with a frequency ω_{osc} ; see Eq. (17)] and (b) the pairwise interaction force F_{int} [cf. Eq. (24)] from other dark-bright solitons. Thus, taking into account that $F_{tr} = -\omega_{osc}^2 x_0$ [16], one may write the

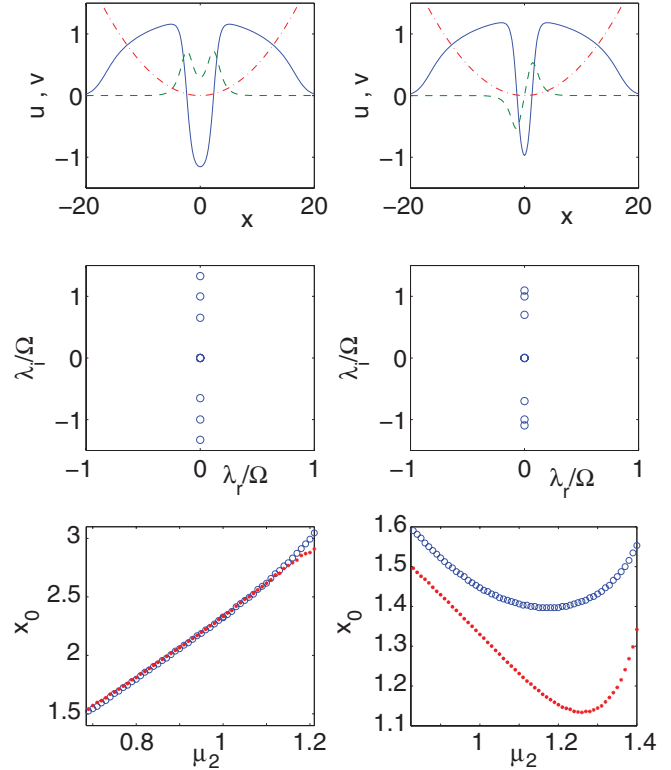


FIG. 4. (Color online) The left and right columns correspond, respectively, to an in-phase and an out-of-phase dark-bright-soliton pair in a harmonic trap with $\Omega = 0.1$. The top row of panels depicts the profiles of the DB-soliton pairs (solid blue lines and dashed green lines correspond, respectively, to the dark and bright components) and the trapping potential (dashed-dotted red line). The middle row of panels depicts the spectral plane (λ_r, λ_i) rescaled by the trap frequency Ω . The bottom row of panels depicts the numerical (small red stars) and the analytical (blue circles) results for the equilibrium distance between the solitons as a function of μ_2 ; the theoretical prediction is based on Eq. (27).

effective equation of motion for the center x_0 of a two-DB-soliton state as follows:

$$\ddot{x}_0 = F_{tr} + F_{int}. \quad (27)$$

One can thus straightforwardly generalize the above equation for \mathcal{N} -interacting DB-soliton states, similar to the case of multiple dark solitons in one-component BECs [13,14,38].

Importantly, the presence of the trap allows for the existence of stationary DB-soliton molecules not only for out-of-phase bright solitons (as in the homogeneous case) but also for in-phase bright solitons. In the latter case, the repulsion between both the dark- and the bright-soliton components is balanced by the trap-induced restoring force F_{tr} . In the case of two-DB solitons placed at $x = \pm x_0$, the equilibrium points x_{eq} can readily be found (as before) as solutions of the transcendental equation resulting from Eq. (27) for $\ddot{x}_0 = 0$ in both the in- and out-of-phase cases. To study the stability of these equilibrium points in the framework of Eq. (27), we may again use the ansatz $x_0(t) = x_{eq} + \delta(t)$, and we obtain a linear equation for the small-amplitude perturbation $\delta(t)$, similar to

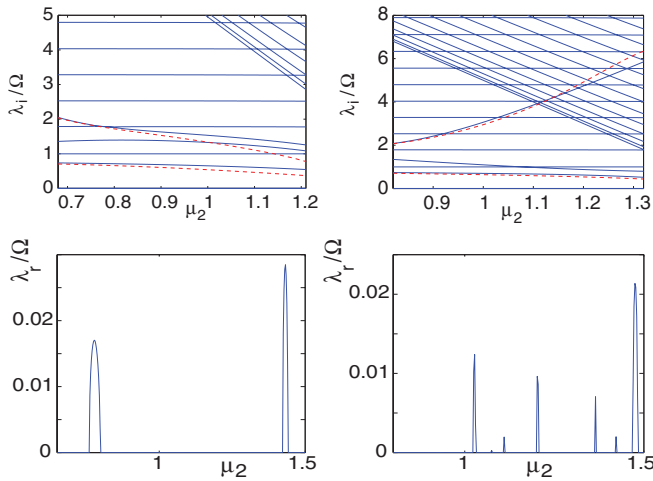


FIG. 5. (Color online) The left and right columns of panels correspond, respectively, to an in-phase and an out-of-phase dark-bright-soliton pair in a harmonic trap with $\Omega = 0.1$. Shown are the imaginary (top row of panels) and the real (bottom row of panels) parts of the eigenvalues as functions of μ_2 for $\mu_1 = 3/2$. In the top panels, the theoretical predictions for the eigenfrequencies of the anomalous modes of the system, pertaining to the in-phase (ω_2) and out-of-phase (ω_1) oscillations of the DB solitons [see Eqs. (28) and (29)], are depicted by dashed red lines. Notice that collisions of modes (eigenvalue crossings) observed in the top panels indicate the emergence of instability windows observed in the bottom panels. The instabilities are of the Hamiltonian-Hopf type and result in the emergence of eigenvalue quartets.

that of Eq. (25), namely, $\delta + \omega_1^2 \delta = 0$, where the frequency ω_1 is given by

$$\omega_1^2 = \omega_{\text{osc}}^2 + \omega_0^2, \quad (28)$$

where ω_0 is given by Eq. (26). Similar to the case of dark solitons in one-component BECs [14] (see also Ref. [4]), by construction, this mode captures the out-of-phase motion of the DB-soliton pair. Furthermore, by symmetry, the in-phase oscillation of the DB-soliton pair in the trap will be performed with the frequency

$$\omega_2 = \omega_{\text{osc}}. \quad (29)$$

These two characteristic frequencies (ω_1, ω_2) coincide with the eigenfrequencies of the two anomalous modes of the BdG spectrum of the trapped DB-soliton pair.

We now turn to a systematic numerical investigation of the above features and of the multiple-DB-soliton states. At first, we consider the two-DB-soliton state in the trap, results for which are summarized in Figs. 4 and 5, both for the in-phase and the out-of-phase configurations. In particular, the top left and right panels of Fig. 4 show examples of an in-phase and an out-of-phase stationary DB-soliton pair, respectively (both for $\mu_1 = 3/2$ and $\mu_2 = 1$). The two middle panels illustrate the corresponding spectral planes, showcasing the linear stability of these configurations. The bottom panels of Fig. 4 show the equilibrium positions of the soliton centers. In the in-phase case (bottom left panel), it is observed that larger chemical potential (number of atoms) in the second component leads to stronger repulsion and hence larger distance from the trap cen-

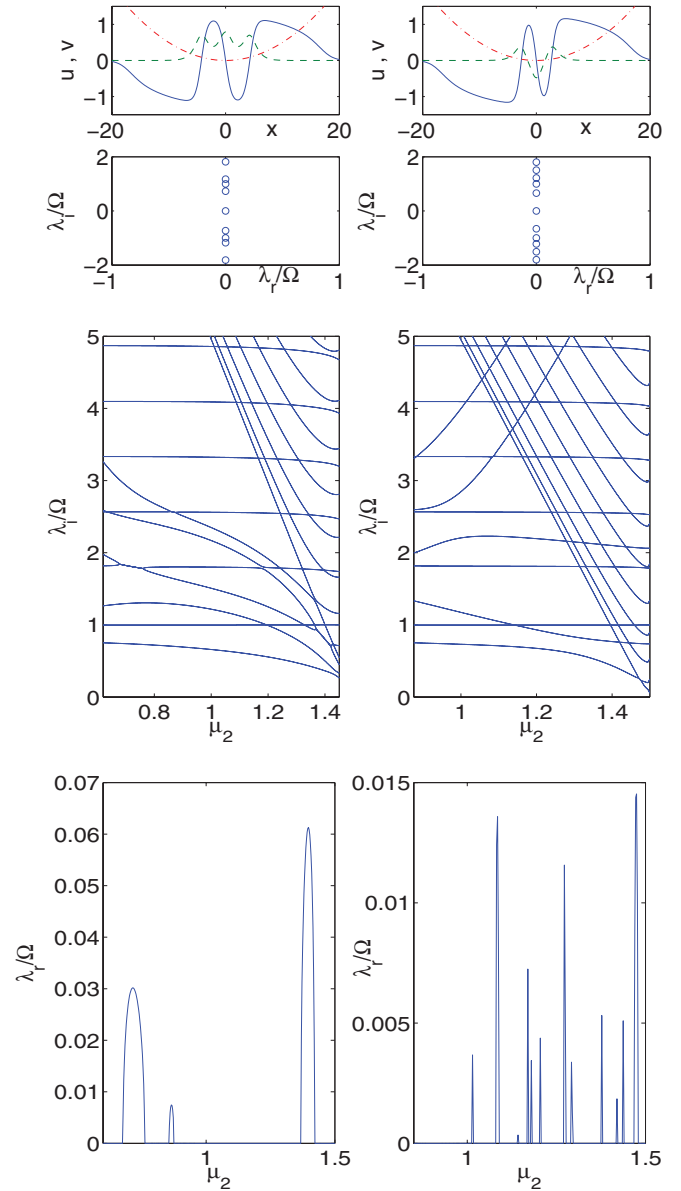


FIG. 6. (Color online) The left and right columns of panels correspond, respectively, to in-phase and out-of-phase three-DB-soliton configurations. The first row of panels depicts the respective stationary states for $\mu_1 = 3/2$, $\mu_2 = 1$, and $\Omega = 0.1$; solid blue lines depict the dark-soliton components, dashed green lines depict the bright ones, and the dash-dotted red line shows the harmonic trap. The second row of panels depicts the spectral planes for the above stationary states, and the third and fourth rows are equivalent to those of Fig. 5, but for the three-DB-soliton configurations.

ter. In the out-of-phase case (bottom right panel), we observe a similar effect but in the reverse direction (due to the attraction of the out-of-phase bright-soliton components) for smaller values of the chemical potential. Notice that in both cases a good agreement is observed between the numerically observed equilibrium separations and the theoretically predicted ones from Eq. (27).

To study the validity of Eq. (28), which is pertinent to small-amplitude oscillations around the fixed points, we show in Fig. 5 the eigenvalues λ of the excitation spectrum

[both for the in-phase (left column) and for the out-of-phase (right column) cases] as functions of μ_2 . The imaginary and real parts, λ_i and λ_r , of the respective eigenvalues, normalized over the trap strength Ω , are respectively shown in the top and bottom panels of Fig. 5. In the top panels, it is straightforward to compare the analytical result of Eq. (28) with the BdG result, namely, the second anomalous mode of the spectrum, corresponding to the out-of-phase oscillations of the DB-soliton pair. Once again, good agreement is observed between the two; the differences may be partially attributed to the “interaction” (i.e., collisions) of these modes with other modes of the BdG spectrum. It is clear from the comparison of the corresponding columns that there exist narrow instability windows, arising due to the crossing of the anomalous mode(s) of the DB-soliton pair with eigenmodes of the background of the two-component system. These instabilities arise in the form of Hamiltonian-Hopf bifurcations [39] through the emergence of quartets of complex eigenvalues resulting from the collision of two pairs. The growth rates of the pertinent oscillatory instabilities are fairly small (i.e., the instabilities are weak) in both the in- and out-of-phase cases; it should be noted, however, that in the latter case, the formation of the quartets appears to be occurring in very narrow intervals.

Naturally, the above considerations can also be generalized to three or more DB solitons, although the analytical calculations become increasingly more tedious; again, as we will show below, in-phase or out-of-phase configurations are possible in the presence of the trap. Pertinent examples, showing two different three-DB-soliton configurations, are illustrated in Fig. 6. In particular, the left column in Fig. 6 corresponds to the in-phase three-DB-soliton state, while the right column corresponds to the out-of-phase variant thereof. In the case under consideration, there exist narrow parametric intervals of dynamical instability, which are narrower for the out-of-phase case (as in the case of the two-DB-soliton states). We should mention, in passing, that the dynamics of two- and three-DB-soliton configurations was recently studied in Ref. [26]; our study complements the latter by yielding analytical approximations and a numerical continuation and bifurcation approach toward such states.

V. CONCLUSIONS AND DISCUSSION

In the present work, we have studied multiple quasi-one-dimensional dark-bright solitons in atomic Bose-Einstein condensates. Our theoretical results were motivated and supported by the experimental evidence of the formation of DB-soliton clusters in a two-component, elongated rubidium condensate, confined in a harmonic trap. The theoretical analysis was based on the study of two coupled one-dimensional Gross-Pitaevskii equations.

Starting from the case of a homogeneous condensate (i.e., in the absence of a trapping potential), we have employed a Hamiltonian perturbation theory to analyze the interaction between two DB solitons. Assuming that the DB solitons are of low velocity and sufficiently far from each other, we have found approximate expressions for the interaction forces between the same or different soliton components. In this way, we derived a classical equation of motion for the center of mass of the DB-soliton pair and revealed the role of the phase

difference between the bright-soliton components: we have shown, in particular, that the repulsion between the dark soliton components may be counterbalanced by the attraction between out-of-phase bright components, thus inducing the existence of stationary DB-soliton pairs even in the case when the external trapping potential is absent. We have found the equilibrium distance between the two DB solitons that compose the stationary DB-soliton pair, with the semianalytical result being in excellent agreement with the relevant numerical one. Additionally, we have demonstrated the linear stability of these stationary DB-soliton pairs by means of analytical and numerical techniques (the latter were based on a Bogoliubov–de Gennes analysis). It was shown that the analytical result for the oscillation frequency of small-amplitude perturbations around the equilibrium distance is in excellent agreement with the pertinent eigenvalue characterizing the frequency of the out-of-phase motion of the DB-soliton pair.

We have then studied multiple DB solitons in the trap. In this case, we have employed a simple physical picture, where the total force acting on the DB solitons was decomposed to an interaction force (derived in the homogeneous case) and a restoring force induced by the trapping potential; the relevant characteristic frequency associated with the latter was the oscillation frequency of a single DB soliton in the trap (which was found to coincide with the pertinent anomalous-mode eigenvalue of the single-DB-soliton system). Following this approach, we were able to find stationary in-trap DB-soliton pairs even in the case where the bright-soliton components were repelling each other: in this case, the trap-induced restoring force was able to counterbalance the repulsive forces between the dark- and bright-soliton components. The semianalytical results for the equilibrium distance and the oscillation frequencies (for the in- and out-of-phase bright-component cases) were again found to be in very good agreement with the respective numerical results, including the anomalous-mode eigenfrequencies pertaining to the in- and out-of-phase motion of solitons. The stability analysis of the DB solitons in the trap indicated the possibility of the existence of unstable modes through Hamiltonian-Hopf instability quartets, although the latter would typically only arise over narrow parametric intervals and with rather weak instability growth rates. Results pertaining to three DB solitons in the trap were presented as well; the main features of these states were found to be qualitatively similar to the ones of the DB-soliton pairs. The identified robustness of such DB-soliton molecules in our analytical and numerical results is in line with the frequent and persistent occurrence of such clusters also in the experiment (although in the latter it is not as straightforward to prepare such “distilled” molecular states).

It would be particularly interesting to further explore the dynamics of multiple-DB-soliton complexes and, potentially, the formation of “DB-soliton gases” comprising such interacting atomic constituents. Deriving Toda-lattice-type equations describing such gases and identifying their stationary states, excitations, and (mesoscopic) solitons (as in the case of single-component dark solitons [38]) are challenges for future work. Another possibility is to extend the present considerations to the vortex-bright solitons found in Ref. [28]. There, it would be relevant to identify whether molecular states consisting of two or three vortex-bright solitons can be constructed and whether

the relative phases of 0 and π between the bright components can still yield different stationary states. Relevant studies are presently in progress.

ACKNOWLEDGMENTS

P.G.K. acknowledges support from the NSF, Grant No. NSF-DMS-0806762, and from the Alexander von Humboldt Foundation. The work of D.J.F. was partially supported by the Special Account for Research Grants of the University of Athens. R.C.G. gratefully acknowledges support from the NSF, Grant No. NSF-DMS-0806762. P.E. acknowledges support from the NSF and ARO.

APPENDIX : THE INTERACTION ENERGIES AND FORCES

The interaction energies E_{DD} , E_{BB} , and E_{DB} are given by the following (approximate) expressions:

$$E_{DD} = 16 \cos^2 \phi \left[\frac{1}{3} D \cos^2 \phi + D + 2(\cos^2 \phi - D^2)x_0 - \frac{3 + 4 \cos^2 \phi}{3D} \cos^2 \phi \right] e^{-4Dx_0}, \quad (\text{A1})$$

$$E_{BB} = \chi \{ 2D[D(1 - Dx_0) - k^2x_0] + D\chi \} \cos \Delta\theta e^{-2Dx_0} + \chi[\chi D(2Dx_0 - 1)(1 + 2 \cos^2 \Delta\theta)]e^{-4Dx_0}, \quad (\text{A2})$$

$$E_{DB} = -4\chi \cos^2 \phi \cos \Delta\theta e^{-2Dx_0} + \chi \cos^2 \phi \left(\frac{16}{3} \cos^2 \phi - 16Dx_0 + 8 \right) e^{-4Dx_0}, \quad (\text{A3})$$

where terms of order $O(e^{-6Dx_0})$ and higher have been neglected (nevertheless, it has been checked that their contribution does not alter the main results that were presented herein). On the other hand, the interaction forces F_{DD} , F_{BB} , and F_{DB} have the following form:

$$F_{DD} = \frac{1}{\chi_0} \left[\frac{1}{3} (544 - 352D_0^2) + 128D_0(D_0^2 - 1)x_0 \right] \times e^{-4D_0x_0}, \quad (\text{A4})$$

$$F_{BB} = \frac{\chi}{\chi_0} \left[-6D_0 + 4D_0^2x_0 - 2\chi \right] D_0^2 \cos \Delta\theta e^{-2D_0x_0} + \frac{\chi^2}{\chi_0} [(1 + 2 \cos^2 \Delta\theta)(-8D_0x_0 + 6)] \times D_0^2 e^{-4D_0x_0}, \quad (\text{A5})$$

$$F_{DB} = \frac{\chi}{\chi_0} [8D_0 \cos \Delta\theta] e^{-2D_0x_0} + \frac{\chi}{\chi_0} \left[-\frac{208}{3} + 64D_0x_0 \right] D_0 e^{-4D_0x_0}, \quad (\text{A6})$$

where $D(t) \approx D_0$ since we are assuming that $\dot{D}(t) \approx 0$.

-
- [1] P. G. Kevrekidis, D. J. Frantzeskakis, and R. Carretero-González, *Emergent Nonlinear Phenomena in Bose-Einstein Condensates: Theory and Experiment* (Springer, Heidelberg, 2008).
- [2] R. Carretero-González, D. J. Frantzeskakis, and P. G. Kevrekidis, *Nonlinearity* **21**, R139 (2008).
- [3] F. Kh. Abdullaev, A. Gammal, A. M. Kamchatnov, and L. Tomio, *Int. J. Mod. Phys. B* **19**, 3415 (2005).
- [4] D. J. Frantzeskakis, *J. Phys. A* **43**, 213001 (2010).
- [5] S. Burger, K. Bongs, S. Dettmer, W. Ertmer, K. Sengstock, A. Sanpera, G. V. Shlyapnikov, and M. Lewenstein, *Phys. Rev. Lett.* **83**, 5198 (1999).
- [6] J. Denschlag *et al.*, *Science* **287**, 97 (2000).
- [7] Z. Dutton, M. Budde, C. Slowe, and L. V. Hau, *Science* **293**, 663 (2001).
- [8] B. P. Anderson, P. C. Haljan, C. A. Regal, D. L. Feder, L. A. Collins, C. W. Clark, and E. A. Cornell, *Phys. Rev. Lett.* **86**, 2926 (2001).
- [9] K. Bongs, S. Burger, S. Dettmer, D. Hellweg, J. Arlt, W. Ertmer, and K. Sengstock, *C. R. Acad. Sci. Paris* **2**, 671 (2001).
- [10] C. Becker, S. Stellmer, P. Soltan-Panahi, S. Dörscher, M. Baumert, E.-M. Richter, J. Kronjäger, K. Bongs, and K. Sengstock, *Nat. Phys.* **4**, 496 (2008).
- [11] S. Stellmer, C. Becker, P. Soltan-Panahi, E.-M. Richter, S. Dörscher, M. Baumert, J. Kronjäger, K. Bongs, and K. Sengstock, *Phys. Rev. Lett.* **101**, 120406 (2008).
- [12] I. Shomroni, E. Lahoud, S. Levy, and J. Steinhauer, *Nat. Phys.* **5**, 193 (2009).
- [13] A. Weller, J. P. Ronzheimer, C. Gross, J. Esteve, M. K. Oberthaler, D. J. Frantzeskakis, G. Theocharis, and P. G. Kevrekidis, *Phys. Rev. Lett.* **101**, 130401 (2008).
- [14] G. Theocharis, A. Weller, J. P. Ronzheimer, C. Gross, M. K. Oberthaler, P. G. Kevrekidis, and D. J. Frantzeskakis, *Phys. Rev. A* **81**, 063604 (2010).
- [15] P. Engels and C. Atherton, *Phys. Rev. Lett.* **99**, 160405 (2007).
- [16] Th. Busch and J. R. Anglin, *Phys. Rev. Lett.* **87**, 010401 (2001).
- [17] H. E. Nistazakis, D. J. Frantzeskakis, P. G. Kevrekidis, B. A. Malomed, and R. Carretero-González, *Phys. Rev. A* **77**, 033612 (2008).
- [18] Yu. S. Kivshar and G. P. Agrawal, *Optical Solitons: From Fibers to Photonic Crystals* (Academic, San Diego, 2003).
- [19] M. J. Ablowitz, B. Prinari, and A. D. Trubatch, *Discrete and Continuous Nonlinear Schrödinger Systems* (Cambridge University Press, Cambridge, 2004).
- [20] Z. Chen, M. Segev, T. H. Coskun, D. N. Christodoulides, Yu. S. Kivshar, and V. V. Afanasjev, *Opt. Lett.* **21**, 1821 (1996).
- [21] E. A. Ostrovskaya, Yu. S. Kivshar, Z. Chen, and M. Segev, *Opt. Lett.* **24**, 327 (1999).
- [22] C. Hamner, J. J. Chang, P. Engels, and M. A. Hoefer, *Phys. Rev. Lett.* **106**, 065302 (2011).
- [23] M. A. Hoefer, J. J. Chang, C. Hamner, and P. Engels, *Phys. Rev. A* **84**, 041605R (2011).
- [24] S. Middelkamp, J. J. Chang, C. Hamner, R. Carretero-González, P. G. Kevrekidis, V. Achilleos, D. J. Frantzeskakis, P. Schmelcher, and P. Engels, *Phys. Lett. A* **375**, 642 (2011).

- [25] S. Rajendran, P. Muruganandam, and M. Lakshmanan, *J. Phys. B* **42**, 145307 (2009).
- [26] C. Yin, N. G. Berloff, V. M. Pérez-García, D. Novoa, A. V. Carpentier, and H. Michinel, *Phys. Rev. A* **83**, 051605(R) (2011).
- [27] A. Alvarez, J. Cuevas, F. R. Romero, and P. G. Kevrekidis, *Phys. D* **240**, 767 (2011).
- [28] K. J. H. Law, P. G. Kevrekidis, and L. S. Tuckerman, *Phys. Rev. Lett.* **105**, 160405 (2010).
- [29] Notice that the numerical results do not significantly change in the case of unequal a_{11} ; however, the analytical calculations and formulas given herein are considerably more involved.
- [30] S. V. Manakov, *Zh. Eksp. Teor. Fiz.* **65**, 505 (1973) [*Sov. Phys. JETP* **38**, 248 (1974)].
- [31] Yu. S. Kivshar and W. Krolikowski, *Opt. Commun.* **114**, 353 (1995).
- [32] P. O. Fedichev, A. E. Muryshv, and G. V. Shlyapnikov, *Phys. Rev. A* **60**, 3220 (1999); A. E. Muryshv, H. B. van Linden van den Heuvell, and G. V. Shlyapnikov, *ibid.* **60**, R2665 (1999); G. Theocharis, P. G. Kevrekidis, M. K. Oberthaler, and D. J. Frantzeskakis, *ibid.* **76**, 045601 (2007).
- [33] N. S. Manton, *Nucl. Phys. B* **150**, 397 (1979); J. P. Gordon, *Opt. Lett.* **8**, 596 (1983); P. G. Kevrekidis, A. Khare, and A. Saxena, *Phys. Rev. E* **70**, 057603 (2004).
- [34] W. Zhao and E. Bourkoff, *Opt. Lett.* **14**, 1371 (1989).
- [35] This result stems from the fact that the coefficients of the terms $\propto \cos \Delta\theta$ in Eqs. (A5) and (A6) are positive definite since the parameter $D_0 \geq 1$ for every $\chi > 0$.
- [36] The interaction between dark and bright solitons does not alter qualitatively (although it obviously affects quantitatively) this interplay between repulsive terms $\propto \exp(-4D_0x_0)$ and attractive ones $\propto \exp(-2D_0x_0)$ (if $\Delta\theta = \pi$).
- [37] R. Radhakrishnan and K. Aravinthan, *J. Phys. A* **40**, 13023 (2007).
- [38] M. P. Coles, D. E. Pelinovsky, and P. G. Kevrekidis, *Nonlinearity* **23**, 1753 (2010).
- [39] J.-C. van der Meer, *Nonlinearity* **3**, 1041 (1990).